X-ray Observations in the Spray Near-Field using Synchrotron X-rays

Theodore J. Heindel*, Danyu Li, Timothy B. Morgan, and Julie K. Bothell
Department of Mechanical Engineering
Iowa State University
Ames, IA 50011-2161 USA

Alberto Aliseda and Nathanael Machicoane
Department of Mechanical Engineering
University of Washington
Seattle, WA 98195-2600 USA

Alan L. Kastengren
X-Ray Science Division, Advanced Photon Source
Argonne National Laboratory
9700 S. Cass Ave., Argonne, IL 60439

Abstract

The ability to control spray formation and dispersion is extremely important to many spray applications such as combustion systems, coating and painting methods, 3D printing processes, and fire suppression designs. The ultimate outcome of our ONR Multidisciplinary University Research Initiative (MURI) project is to demonstrate multiphysics control of liquid sprays issuing from airblast atomizers through the novel integration of advanced diagnostics and the application of data- and simulation-driven model reduction in easy-to-implement control algorithms. Some of the advanced diagnostics used in this project to better understand spray formation include: (1) 2D X-ray radiography and 3D X-ray computed tomography obtained from common tube X-ray sources, and (2) high-speed 2D radiographic movies and detailed 2D density projections from high intensity white beam and focused beam radiography from a synchrotron X-ray source. All of these techniques will focus on imaging the near-field region of the spray. This paper will provide initial X-ray spray imaging observations that were recently recorded using the Advanced Photon Source (APS) at Argonne National Laboratory.

Initial high-speed X-ray images from an airblast atomizer are presented, where the inner liquid flow is laminar (Re_l = 1000) and the outer air flow is turbulent (Re_g = 16,700), with and without gas swirl. Radiographic movies of the atomizer show a very dynamic near-field region, including bag formation and stable air bubble formation inside liquid drops. When air swirl is added, the liquid stream is very unstable near the nozzle exit. A discussion of the quantitative measures that can be acquired from the qualitative white beam images and focused beam radiographic measurements will also be provided. Eventually, these data will be compared to near-field simulations performed at Cornell University and to mid-field measurements completed at the University of Washington – Seattle using an identical flow system.

* Corresponding author, theindel@iastate.edu

Introduction

The ability to control spray formation and dispersion is extremely important to many spray applications, including coating and painting, fire suppression, agricultural weed and pest control, and liquid fuel combustion. Spray regions are generally identified as near-field, mid-field, and far-field, with the demarcation between regions being nebulous. The near-field region is closest to the nozzle exit and may contain a liquid sheet that forms bags and undergoes breakup, leading to ligament and drop formation. Depending on the type of nozzle and operating conditions, liquid sheet formation and breakup may be observed or happen right at the nozzle exit. The nozzle could also have a liquid core that dissipates as the liquid is atomized [1].

Spray characteristics can easily be assessed in the mid- and far-field regions, well after liquid sheet (or liquid core) breakup and droplet formation, using various optical/laser diagnostic techniques [2]. The conditions in the near-field region can influence mid- and far-field characteristics; however, near-field measurements are extremely challenging because the spray in this region is typically optically dense, rendering optical/laser diagnostics largely ineffective.

Synchrotron radiation, like the Advanced Photon Source (APS) at Argonne National Laboratory, can provide a high-flux, monochromatic X-ray beam that can be used to provide high spatial and temporal resolution of the spray. The APS has been used by several researchers to image the near-field of a spray using focused beam radiographic imaging and X-ray phase contrast imaging. Many citations of this work can be found in a recent review covering synchrotron flow visualization [3].

The 7-BM beamline at APS has recently been upgraded to provide high intensity broadband X-rays that can be used for 2D radiographic imaging with microsecond or sub-microsecond time resolution [4]. It is called white beam imaging because the high intensity continuous wave beam is composed of a range of X-ray energies (wavelengths) that can produce very detailed 2D spatially and temporally resolved measurements of highly dynamic 3D events, like spray formation.

This paper will describe the use of the white beam imaging system at APS as applied to an airblast atomizer operated at a liquid Reynolds number of $Re_l = 1000$ and gas Reynolds number of $Re_g = 16{,}700$, with and without gas swirl.

Experimental Setup

Figure 1 provides a schematic of the experimental flow loop used in this study, while Figure 2 provides a picture of the airblast atomizer arrangement mounted in the 7-BM beam line at APS. The nozzle is identical to the one used by the University of Washington in their optical flow visualization studies [5], but mounted vertically so the jet exits the nozzle in the direction of gravity; this orientation will also be used when the nozzle and flow loop are mounted in the Iowa State University XFloViz facility [6] and imaged with broadband X-rays produced with tube sources [7-9].

The aluminum airblast nozzle design and assembly are provided elsewhere [5] so details will not be given here. For the nozzle used in this study, the actual water nozzle ID and OD are 2.1 mm and 2.7 mm, respectively. The water nozzle is centrally located inside the air nozzle with an ID of 10 mm.

An 18.9 L (5 gal) water tank is filled with distilled water and pressurized with compressed air to provide a constant volumetric flow rate in the inner nozzle. Water exited the tank, passed through a manual ball valve, electronic proportioning (control) valve, and flow meter before entering a plenum on top of the nozzle and then exited the nozzle. The flow rate was held constant at 0.099 L/min using LabView and a simple PID control loop. The water jet exit velocity was 0.48 m/s and the Reynolds number was $Re_l = 1000$, forming a laminar water jet.

Compressed air was used as the gas stream in the airblast atomizer. The air was first filtered and then divided into two streams. One stream (co-flow air) passed through a manual ball valve, electronic proportioning valve, and flow meter before being divided into four streams that uniformly entered a converging nozzle perpendicular to the inner water nozzle. A second stream (swirl air) passed through a separate manual ball valve, electronic proportioning valve, and flow meter before being divided into four streams that uniformly entered the converging nozzle tangentially to provide swirl if desired. The co-flow and swirl air streams were held constant at their desired flow rates using LabView and a simple PID control loop for each stream.

For the cases in this initial study, the total gas flow rate was fixed at 150 SLPM. For the no-swirl conditions, the swirl air line was closed and all the air entered the nozzle through the co-flow lines, producing a nominal co-flow air exit velocity of 34 m/s and a gas Reynolds numbers (based on hydraulic diameter) of $Re_g = 16{,}700$. In the case of imposed swirl, the gas flow rate was 100 or 75 SLPM through the co-flow line and 50 or 75 SLPM through the swirl line, producing a swirl ratio of SR = 0.5 or 1.

The atomized water jet was injected into the imaging region before being expelled into an exhaust system. The exhaust system used the building ventilation to pull low-velocity ambient air into the exit stream to prevent recirculation of the atomized spray.

The 7-BM beamline at APS was used in this study. It was configured similarly to that used by Radke [10] in his white beam studies. Because of the intensity of the white beam (~0.6 W/mm^2), measures are needed to avoid heating of the experimental equipment. During an experiment, the beam passed through a rotating chopper wheel

to reduce the average power of the beam. The chopper wheel is composed of two 15.2 cm diameter, 6.35 mm thick copper discs with two "pie wedge" openings cut into each disc. The discs were arranged such that a common open wedge of about 7.9° was used. The discs were spun at 0.5 Hz, yielding a burst of x-rays at 1 Hz.

After the chopper wheel, the beam passed through the spray region and then encountered a 500 μm thick YAG:Ce scintillator crystal, which fluoresced in the visible spectrum with an intensity proportional to the X-ray intensity. The image on the scintillator was reflected to a high-speed camera via a 45° mirror. The high-speed camera was a Photron FASTCAM Mini AX50 with 2000 fps at a full field of view (1024 × 1024 pixels). However, images in this study were acquired at 6000 fps at a reduced field of view. The camera was connected to 105 mm – 50 mm lens combination providing an effective magnification of 2.1x. Additionally, lead-containing shielding was placed around the imaging equipment to shield it from scattered X-rays.

Finally, because the white beam was not square (it was wider than tall) and the intensity varied from the beam center, flatfield images in which no spray was present were acquired at each spatial location, and then subtracted from the raw image frames.

Results

Figure 3 shows three images taken at the nozzle exit with Re_l = 1000, Re_g = 16,700, and SR = 0, 0.5, and 1. In all images, the liquid nozzle tip is faintly recorded and shows a slight asymmetrical chamfer, as shown in the enhanced magnified view. The liquid nozzle wall locations are identified with markers because they are difficult to identify without magnifying the image. Also, although the nozzle was designed to be 2 mm ID and 3 mm OD [5], the actual nozzle dimensions, as measured in the radiographs, was 2.1 mm ID and 2.7 mm OD. These are critical dimensions that must be matched by high-resolution simulations to obtain meaningful validation of the simulations, which will be performed at Cornell University [11]. The resolution afforded by the X-ray images allows for a direct, high-resolution validation of the measurements.

With the no swirl condition (Image 3a), the liquid jet exits the inner nozzle and undulates slightly in a helical pattern. Note that the water wets the nozzle tip. It is also interesting that periodically, the water wicks up the outside of the nozzle tip by 1 mm or more. These features of the liquid-gas interface represent important boundary conditions for high-resolution modeling efforts. Instabilities periodically form along the gas-liquid interface in which it appears that gas tries to penetrate the liquid, forming a bag (identified in Image 3a). The bag grows and deforms the liquid jet, leading to ligament formation and eventually droplets (which appear much further downstream).

When SR = 0.5 with the total gas flow rate held constant (Image 3b), bag and ligament formation occur much closer to the nozzle tip and the liquid region substantially deforms.

When SR = 1 with the total gas flow rate held constant (Image 3c), liquid bags break near the nozzle exit. As the gas swirls around the liquid stream, video playback shows the bag breakup occurring in multiple directions. For example, the bag breakup identified in Image 3c occurs from the lower right to the upper left in the image and then the droplets are diverted downward.

Figure 4 shows selected images along the nozzle centerline but downstream of the nozzle exit with Re_l = 1000, Re_g = 16,700, and SR = 0, 0.5, and 1. The nozzle exit plane is identified with the horizontal line and the specific distances to the image centers are identified. When the gas is purely co-flow (SR = 0), the liquid jet is still intact at y = 4.6 mm from the nozzle exit plate, and it undulates with a wider amplitude forming more bags along its surface. Periodically, the liquid film ruptures and reforms, trapping an air bubble inside the liquid (identified in Image 4a). The bubble is easily viewed on a large computer monitor but may be difficult to see in the image unless it is magnified. The increased X-ray transmission inside the bubble (i.e., reduced X-ray absorption) clearly shows that the structures are indeed gas-filled bubbles.

Increasing the swirl ratio to SR = 0.5 while keeping the flow rates constant (Image 4b) reveals the liquid jet is no longer intact at y = 11.6 mm from the nozzle exit plane. Two air bubbles inside the liquid ligaments in Image 4b are identified.

Further increasing the swirl ratio to SR = 1 (Image 4c, y = 6.75 mm from the nozzle exit plane) reveals sheets of liquid passing through the image region. The sheets have several included air bubbles.

In all cases that air bubbles are observed, we believe they are created when a bag forms in the liquid jet and then closes upon itself, which can be confirmed by X-ray video observations of this process. Then, as liquid breakup occurs, some of the bubbles remain trapped in the liquid droplets, forming "hollow droplets" [10]. This is observed with X-ray imaging where air bubbles inside the liquid droplet travel with the liquid. The presence of small bubbles inside the liquid of an atomizing jet has been observed in other studies as well [10, 12].

Future data analysis

The use of the APS source for imaging an airblast atomizer is very useful. In 5 days of data collection, we recorded over 800 GB of data, which will take several months to analyze. The discussion in this paper is from our preliminary analysis, and further details will be forthcoming.

The white beam is not very large (approximately 10 mm × 8 mm), and further reductions in image size

through camera controls allowed for faster frames acquisition rates, so the entire jet exit stream was not captured in a single image (unlike the tube source at ISU [6]). However, several downstream regions were imaged with the white beam source. Each imaging event recorded 39-150 image bursts for a total of 5850 images. The 150 consecutive images corresponded to the length of time the rotating chopper wheel was opened. The pixel intensity can be averaged to obtain an average liquid distribution in the imaging region, and the various imaging regions can be combined to show where the jet, on average, is located. These ensemble images will be compared to average light intensity images acquired at the University of Washington – Seattle using an identical nozzle and flow system [5].

In addition to white beam imaging of several airblast atomizer flow conditions, we also obtained focused beam radiographic measurements of the same conditions. These data will be analyzed to obtain detailed time-average projected mass fractions across the jet at different axial locations, similar to that found in [13-15]. The original data in our testing were obtained at a sampling rate of up to 6.25 MHz for a 10 s period at each measurement location. We plan to complete time series analysis on these data to assess turbulence in the near field region of the atomizer; similar analysis was recently completed by Radke [10] for a very different atomizer design.

Conclusions

White beam synchrotron radiation was used to complete high-speed X-ray imaging of an airblast atomizer operated at $Re_l = 1000$ and $Re_g = 16{,}700$, with swirl ratios of SR = 0, 0.5, and 1. The images show a highly dynamic gas-liquid interface with instabilities that cause the liquid jet to break up closer to the nozzle exit as swirl rate increases. Gas bubbles inside the liquid region we also observed were believed to form when gas penetrates the liquid region, creating bags that close upon themselves, trapping gas bubbles inside the liquid.

Acknowledgements

This work was sponsored by the Office of Naval Research (ONR) as part of the Multidisciplinary University Research Initiatives (MURI) Program, under grant number N00014-16-1-2617. The views and conclusions contained herein are those of the authors only and should not be interpreted as representing those of ONR, the U.S. Navy or the U.S. Government.

This work was performed at the 7-BM beamline of the Advanced Photon Source, a U.S. Department of Energy (DOE) Office of Science User Facility operated for the DOE Office of Science by Argonne National Laboratory under Contract No. DE-AC02-06CH11357.

References

1. Linne, M., "Imaging in the optically dense regions of a spray: A review of developing techniques," *Progress in Energy and Combustion Science*, **39**(5): pp. 403-440, 2013.
2. Fansler, T.D. and Parrish, S.E., "Spray measurement technology: A review," *Measurement Science and Technology*, **26**(1): pp. 34, 2015.
3. Kastengren, A. and Powell, C., "Synchrotron X-ray techniques for fluid dynamics," *Experiments in Fluids*, **55**(3): pp. 1-15, 2014.
4. Halls, B.R., Radke, C.D., Reuter, B.J., Kastengren, A.L., Gord, J.R., and Meyer, T.R., "High-speed, two-dimensional synchrotron white-beam X-ray radiography of spray breakup and atomization," *Optics Express*, **25**(2): pp. 1605-1617, 2017.
5. Machicoane, N. and Aliseda, A., "Experimental characterization of a canonical coaxial gas-liquid atomizer," in *ILASS - Americas 2017: 29th Annual Conference on Liquid Atomization and Spray Systems*, Atlanta, GA, May 15-18, 2017.
6. Heindel, T.J., Gray, J.N., and Jensen, T.C., "An X-ray system for visualizing fluid flows," *Flow Measurement and Instrumentation*, **19**(2): pp. 67-78, 2008.
7. Halls, B.R., Heindel, T.J., Kastengren, A.L., and Meyer, T.R., "Evaluation of x-ray sources for quantitative two- and three-dimensional imaging of liquid mass distribution in atomizing sprays," *International Journal of Multiphase Flow*, **59**(0): pp. 113-120, 2014.
8. Halls, B.R., Morgan, T.B., Heindel, T.J., Meyer, T.R., and Kastengren, A.L., "High-speed radiographic spray imaging with a braodband tube source," in *AIAA Science and Technology Forum and Exposition 2014*, National Harbor, MD, January 13-17, 2014.
9. Meyer, T.R., Schmidt, J.B., Nelson, S.M., Drake, J.B., Janvrin, D.M., and Heindel, T.J., "Three-dimensional spray visualization using X-ray computed tomography," in *ILASS Americas: 21st Annual Conference on Liquid Atomization and Spray Systems*, Orlando, FL, May 18-21, 2008.
10. Radke, C.D., *An investigation of coaxial rocket injector flows using synchrotron X-rays*, PhD Dissertation, Department of Mechanical Engineering, Iowa State University, 2017.
11. Chiodi, R., Vu, L.X., and Desjardins, O., "An exploration of initial destabilization during air-blast atomization using 3D simulations," in *ILASS - Americas 2017: 29th Annual Conference on Liquid Atomization and Spray Systems*, Atlanta, GA, May 15-18, 2017.
12. Lin, K.-C., Rajnicek, C., Mccall, J., Carter, C., and Fezzaa, K., "Investigation of pure- and aerated-liquid jets using ultra-fast X-ray phase contrast imaging,"

Nuclear Instruments and Methods in Physics Research Section A: Accelerators, Spectrometers, Detectors and Associated Equipment, **649**(1): pp. 194-196, 2011.

13. Kastengren, A. and Powell, C.F., "Spray density measurements using X-ray radiography," *Proceedings of the Institution of Mechanical Engineers, Part D: Journal of Automobile Engineering*, **221**(6): pp. 653-662, 2007.
14. Kastengren, A.L., Powell, C.F., Wang, Y., Im, K.-S., and Wang, J., "X-ray radiography measurements of diesel spray structure at engine-like ambient density," *Atomization and Sprays*, **19**(11): pp. 1031-1044, 2009.
15. Kastengren, A.L., Tilocco, F.Z., Duke, D.J., Powell, C.F., Zhang, X., and Moon, S., "Time-resolved X-ray radiography of sprays from engine combustion network spray a diesel injectors," *Atomization and Sprays*, **24**(3): pp. 251-272, 2014.

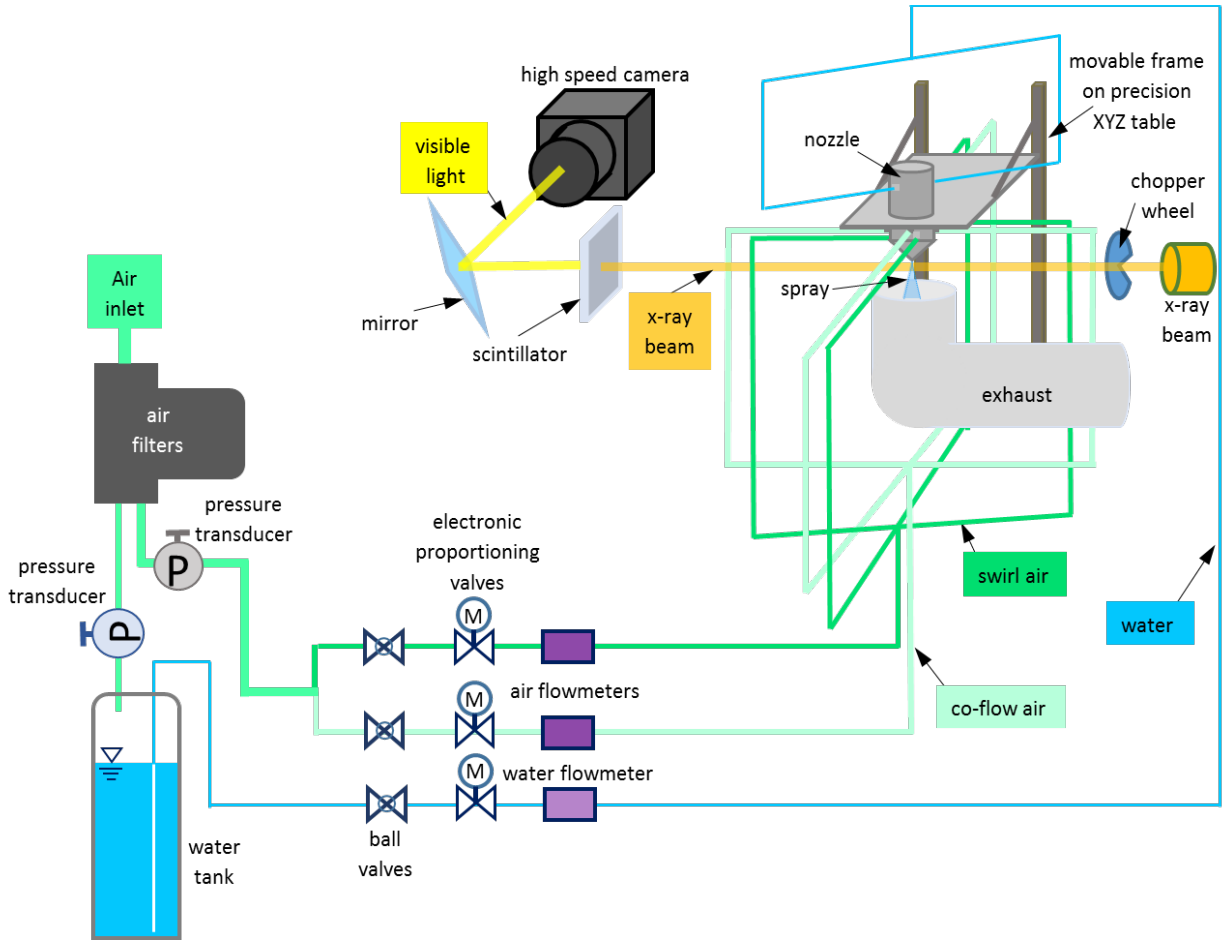

Figure 1. Flow loop used at APS for X-ray imaging of an airblast atomizer.

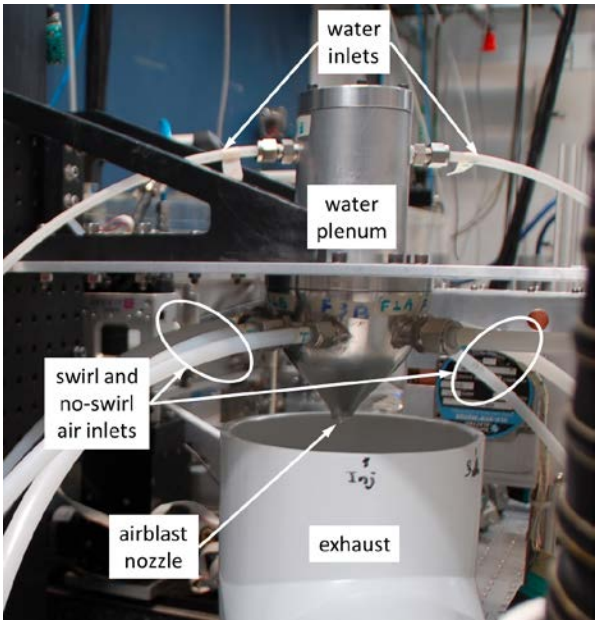

Figure 2. Closeup picture of the airblast atomizer mounted in the 7-BM hutch at APS.

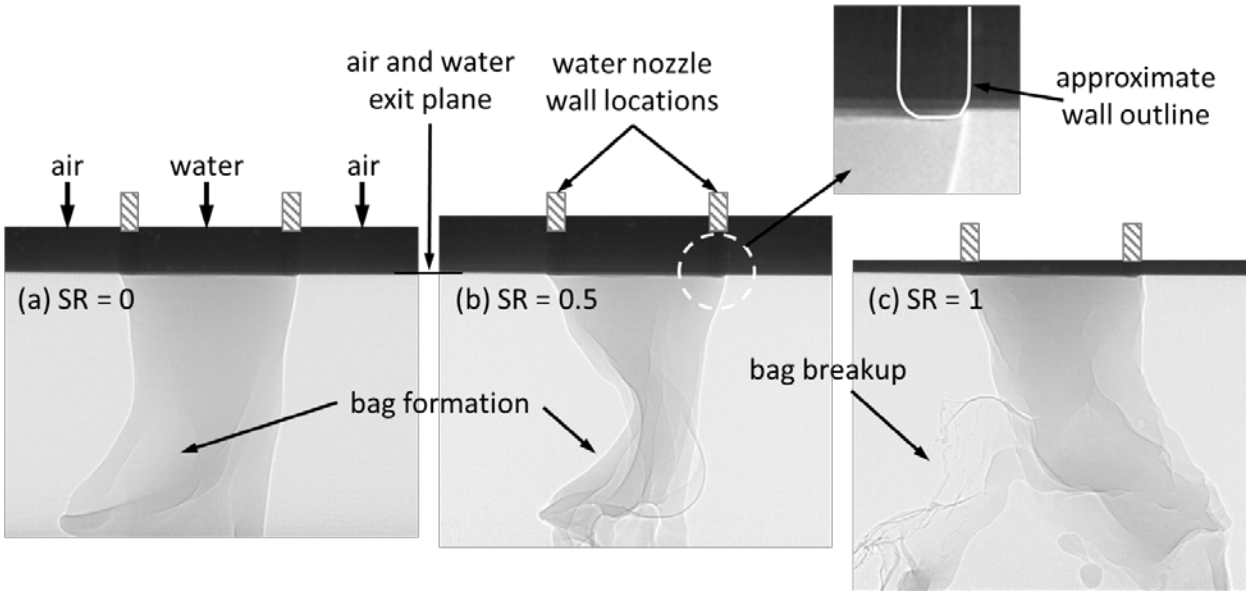

Figure 3. Single radiograph right at the airblast atomizer exit with Re_l = 1000, Re_g = 16,700, and (a) SR = 0 (image size 6.1 mm × 4.6 mm), (b) SR = 0.5 (image size is 5.8 mm × 4.9 mm), and (c) SR = 1 (image size is 5.8 mm × 4.9 mm).

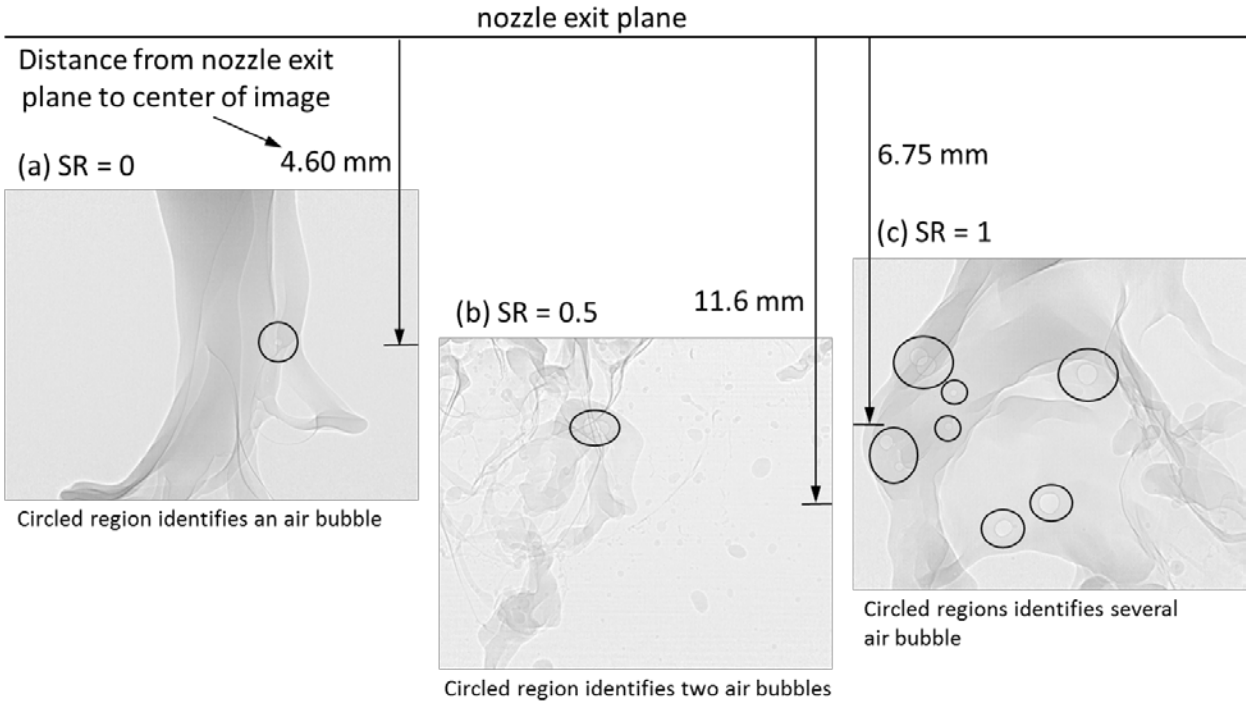

Figure 4. Single radiographs several mm from the airblast atomizer exit along the nozzle centerline with Re_l = 1000, Re_g = 16,700, and (a) SR = 0 (image size 6.1 mm × 4.6 mm), (b) SR = 0.5 (image size is 5.8 mm × 4.9 mm), and (c) SR = 1 (image size is 5.8 mm × 4.9 mm).